

## Counterion-Mediated Hydrogen-Bonding Effects: Mechanistic Study of Gold(I)-Catalyzed Enantioselective Hydroamination of Allenes

Ji Hye Kim, Sung-Woo Park, Sae Rom Park, Sungyul Lee,\* and Eun Joo Kang\*<sup>[a]</sup>

Dedicated to Professor Eun Lee on the occasion of his retirement and 65th birthday

The use of transition metals as unsaturated C–C bond activators toward nucleophilic attack continues to grow exponentially for efficient and atom-economic organic transformations. The majority of nucleophilic additions proceed through the outer-sphere mechanism, that is, *anti* addition to the metal-coordinated C–C multiple bond complexes. However, few alternative inner-sphere mechanisms<sup>[1]</sup> have been proposed, in which the coordination of the nucleophile to the metal is followed by insertion of a C–C multiple bond into the M–Nu bond, such as the Ir,<sup>[2a,b]</sup> Ln,<sup>[2c]</sup> Pd,<sup>[2d]</sup> and Au-catalyzed<sup>[2e–k]</sup> hydrofunctionalization reactions. While the detailed variation of the inner-sphere mechanism highly depends on the electronic and redox character of transition metals, more importantly, these reactions are distinguished by *syn*-stereochemical pathways from the outer-sphere mechanism.

While intensive stereochemical investigations into various kinds of gold(I) catalysis<sup>[3]</sup> suggested the *anti*-addition mechanism, our specific interest began from the significant enantioselectivity in the gold(I)-catalyzed transformations of allenes. Despite a number of reports on transition metal catalyzed addition of heteroatom nucleophiles to allenes,<sup>[4,5]</sup> the asymmetric variants are reported exclusively with the gold catalyst.<sup>[6,7]</sup> This fact stimulates ideas for the perfect role of a gold catalyst in the challenging control of stereoselectivities, especially when substituted allenes are used as substrates. Enantioselective gold(I) catalysis is not restricted to classic  $\pi$ -activation processes. The efficient gold catalyst has

been selected as the form of chiral bis(gold)-phosphine complexes, which could lead to formation of aurophilic Au–Au interactions.<sup>[7]</sup> Another intriguing phenomenon is the pronounced counterion effect that points to the importance of nonbonding interactions between the auxiliary (AuX) group and the reactive gold center. Herein we report a new type of the counterion-directed *syn*-addition pathway in gold-catalyzed hydroamination reactions. In parallel, we have found that the nonbonding interaction between the nucleophile and gold in the pre-reaction complex is the origin of the enantioselectivity of complex allene substrates.

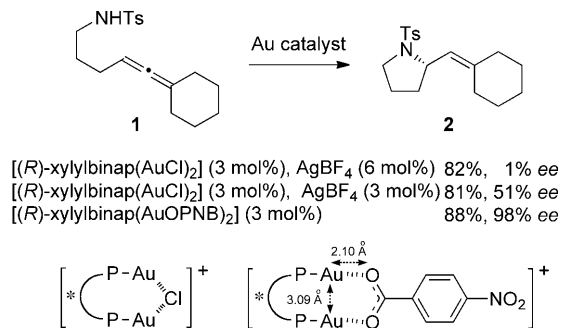
To obtain insight into the possible origins of enantioselectivity in the gold-catalyzed hydroamination reactions, we have carried out both experiments and quantum chemical studies, employing the density functional theory method B3LYP<sup>[9]</sup> with the 6-31G basis set and the effective core potential for Au (Hay–Wadt VDZ),<sup>[10]</sup> as implemented in the Gaussian 09<sup>[11]</sup> set program. Stationary structures are confirmed by ascertaining that all the harmonic frequencies are real. The structure of the transition state is obtained by verifying that one and only one of the harmonic frequencies is imaginary, and also by carrying out the intrinsic reaction coordinate (IRC) analysis along the reaction pathway. Zero point energies (ZPE) are taken into account, and default criteria are used for all optimizations.

Based on the previous observations in the gold-catalyzed enantioselective hydroamination (Scheme 1),<sup>[5b]</sup> the enantioselectivity was concluded to be strongly affected by the remaining counterion coordinated to gold, and the *para*-nitrobenzoate (OPNB) counterion proved to be an ideal one to transfer the chiral information of the 2,2'-bis(diphenylphosphino)-1,1'-binaphthyl (binap) ligand to the relatively distant reaction center. Furthermore, this counterion effect in gold-catalyzed hydroamination was developed and applied by using a chiral 2,2'-dihydroxy-1,1'-binaphthyl (binol)-derived phosphate anion, thus rendering the chiral counterion-mediated transition metal catalysis powerful.<sup>[12]</sup> To check the role of the counterion in the catalytically active species, we

[a] J. H. Kim,<sup>+</sup> S.-W. Park,<sup>+</sup> S. R. Park, Prof. S. Lee, Prof. E. J. Kang  
Department of Applied Chemistry  
Kyung Hee University  
Yongin-si, Gyeonggi-do, 446-701 (Korea)  
Fax: (+82) 31-202-7337  
E-mail: sylee@khu.ac.kr  
ejkang24@khu.ac.kr

[+] These authors contributed equally to this work.

Supporting information for this article is available on the WWW under <http://dx.doi.org/10.1002/asia.201100135>.



Scheme 1. Effect of counterion in the gold(I)-catalyzed enantioselective hydroamination.

looked more closely to the isolated monocationic gold catalyst with the OPNB counterion. In the calculated structure, the  $\text{RCO}_2^-$  anion coordinates in a bidentate fashion to the bis(gold)-phosphine complex with  $\text{Au}-\text{O}$  distances of 2.09 Å and 2.10 Å, respectively; this favors the equilibrium to the monocationic complex by the counterion dissociation.<sup>[6b]</sup> Remarkably, the prominent metallophilic interactions known as aurophilic attraction, are observed between  $\text{Au}^{\cdot\cdot\cdot}\text{Au}$  centers (3.09 Å) and this organized monocationic gold complex is considered as the efficient active catalyst to provide enantioselective reactions.<sup>[13]</sup>

Figure 1 presents the structures and the energy profiles of the pathways towards the *S* and *R* isomers of the hydroamination product. Here, we employ a model reaction without

*N*-tosyl protecting group, after confirming that the omission slightly alters the energetics of profiles,<sup>[14]</sup> although the pathways could vary according to the electronic character of the amine.<sup>[5g]</sup> In the global minimum energy structure, the  $\text{N}-\text{Au}$  distance is quite small ( $\text{R}_{\text{N}-\text{Au}}=2.14$  Å), thus indicating strong interactions between the amino and the gold atom.<sup>[15]</sup> This complex is, however, not amenable to the hydroamination reaction, because the allene moiety is located far from the amino group. The hydroamination reaction begins with the coordination of the allene to the cationic gold catalyst,  $[(R)\text{-binap}(\text{AuOPNB})]\text{Au}^{1+}$ , thus forming the  $\eta^2$  allene-gold complexes described in the pre-reaction complexes. The most characteristic feature of the optimized geometries of pre-reaction complexes is the presence of  $\text{N}-\text{H}\cdots\text{O}$  hydrogen bonding between the amino alkyl chain and the benzoate anion coordinated to gold; this allows nucleophilic attack to occur at the *cis* position to gold, and not from the less hindered opposite side. Despite extensive computational searching, any attempt to find the latter type of pre-reaction complexes failed. We extensively searched over the potential-energy landscape of the present system by designating the initial conformation of the catalyst and the substrate for *anti* addition and letting the system relax to any stationary structure with all real frequencies by the Gaussian optimization algorithm (Figure 2). We have found that no stationary structures are obtained for the *anti*-addition pathway, and that the initial structure drifts down to lower energy towards a post-reaction complex (*S*), as shown in Figure 1.<sup>[16]</sup>

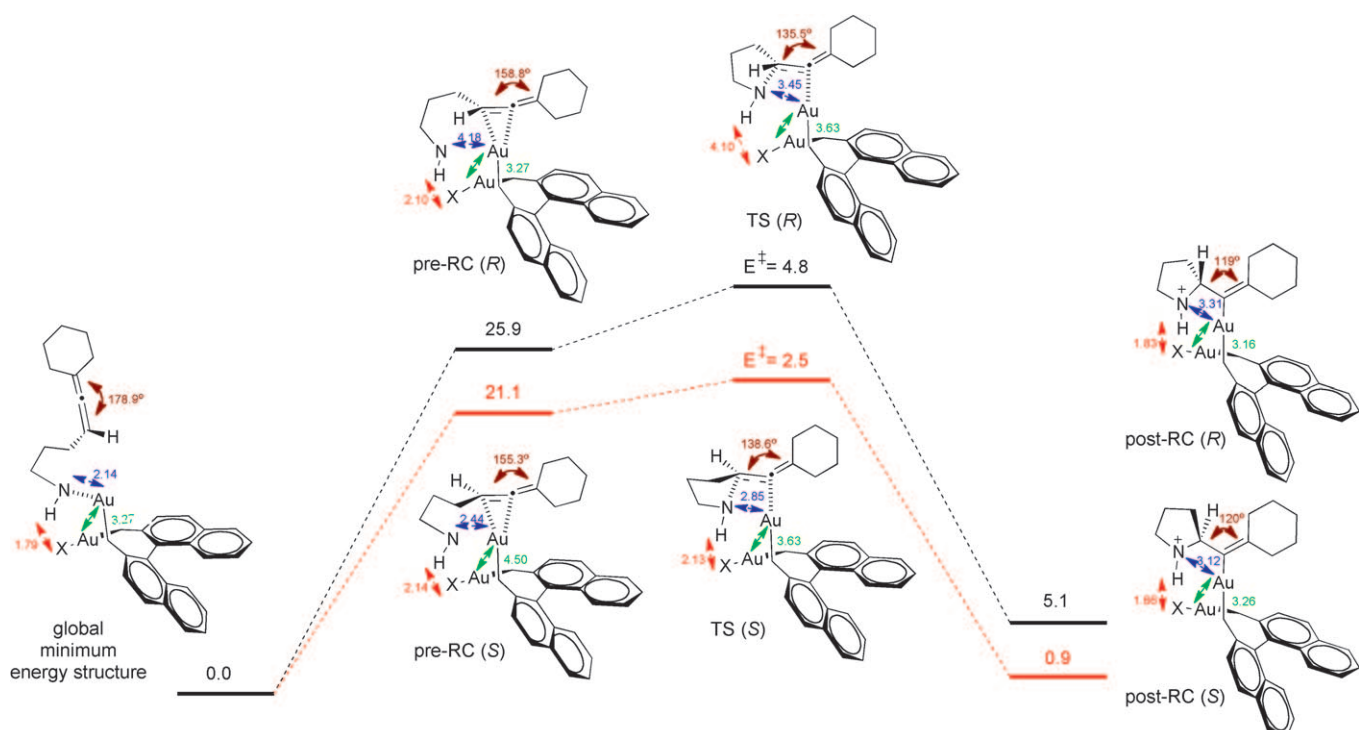


Figure 1. Energy profile for two pathways in the *syn*-addition mechanism. Distances in Å, and relative energies in  $\text{kcal mol}^{-1}$ . pre-RC (*S*) = pre-reaction complex towards the (*S*) isomer, etc., TS = transition state, post-RC = post-reaction complex, X = *para*-nitrobenzoate. Other protons on the amine and phosphine groups are omitted to simplify the figure.

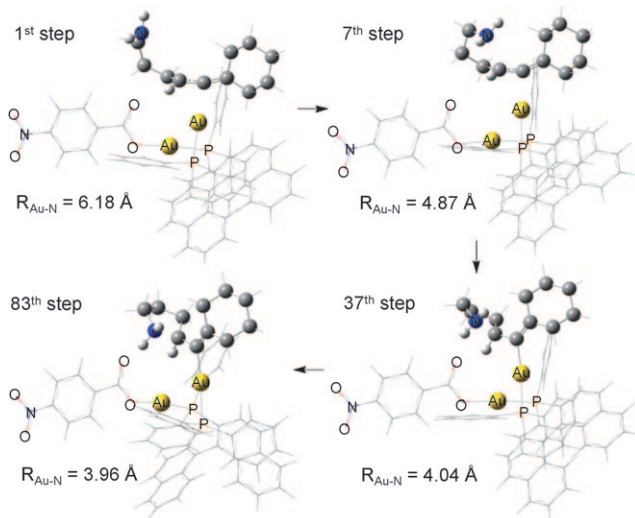


Figure 2. Snapshots from a conformation in which the amino group is located in an *anti* position to the allene.

This structure of the pre-reaction complex may well describe the origin of the observed enantioselectivity. Of the two pre-reaction complexes corresponding to two different coordinating faces of allene, the pre-reaction complex towards the *S* isomer (pre-RC (*S*)) exhibits a much shorter N···Au distance (2.44 Å) than that of pre-RC (*R*) (4.18 Å), because the interactions between the amino alkyl chain and gold are not interfered by the allenic proton in the former structure. The preorganized structure of pre-RC (*S*), calculated to be more stable (energy is lower by 4.8 kcal mol<sup>-1</sup>) than pre-RC (*R*), might result in a lower activation barrier to *S* isomers than the isomeric pathway (2.5 vs 4.8 kcal mol<sup>-1</sup> from the pre-RCs, 23.6 vs 30.7 kcal mol<sup>-1</sup> from the global minimum energy structure). It seems that significant weakening of hydrogen bonding (N–H···O distance increases from 2.10 to 4.10 Å) in the TS (*R*) renders it much less stable than TS (*S*) in which the N–H···O distance remains essentially the same.<sup>[17]</sup> Therefore, the reaction pathway towards the *S* isomer is much more feasible both in the thermodynamic and kinetic sense, in excellent agreement with the experimentally observed enantioselectivity in the hydroamination of allenes. Deprotonation of the post-reaction complex followed by protonolysis of the vinyl gold bond (protodeauration), which is considered to proceed with retention of configuration, is ruled out as the origin of enantioselectivity.<sup>[18]</sup>

To further provide the evidence for this *syn* mechanism, we prepared a number of alkyl-substituted unsymmetric allenes, and applied them to the gold-catalyzed enantioselective hydroamination reactions (Table 1). We envisioned that this difference in spacial environments of allenes would give different effects on the coordinating direction of the gold catalyst. Treating various tosylamides with the binuclear gold catalyst, [(*R*)-binap(AuOPNB)<sub>2</sub>], at 50 °C produced 2-vinyl pyrrolidines with excellent yields, but showed low diastereoselectivity of 2:1 to 3:1 in favor of the *E* isomers.<sup>[19]</sup>

Table 1. Gold(I)-catalyzed enantioselective hydroamination of unsymmetric allenes.<sup>[a]</sup>

<chem>CC(C=CC=C)N(Ts)C(=O)C[C@H](C)C=C</chem>	<chem>[(R)-binap(AuOPNB)2]</chem>	<chem>CC(C=CC=C)N(Ts)C(=O)C[C@H](C)C=C</chem>
<b>3a-d</b>	<b>MeNO<sub>2</sub>, 50 °C</b>	<b>4a-d</b>
<b>4a</b>	<b>4b</b>	<b>4c</b>
<b>4d</b>		<b>4d</b>
<i>E/Z</i> = 2.2:1 83 % yield 93( <i>E</i> ), 80( <i>Z</i> ) % ee	<i>E/Z</i> = 1.5:1 97 % yield 93( <i>E</i> ), 93( <i>Z</i> ) % ee	<i>E/Z</i> = 2.0:1 <sup>[b]</sup> 98 % yield 89( <i>Z</i> ) % ee 79( <i>E</i> ), 89( <i>Z</i> ) % ee 77( <i>E</i> ), 93( <i>Z</i> ) % ee

[a] 5 mol % [(*R*)-binap(AuOPNB)<sub>2</sub>], MeNO<sub>2</sub> (0.3 M), 50 °C, 15 h; Yield of isolated products (*E*+*Z*) after column chromatography. [b] 3 mol % [(*S*)-binap(AuOPNB)<sub>2</sub>].

Although we expected that the *Z* isomers might predominate over *E* isomers, hypothesizing that the gold catalyst would approach from the face of the less hindered methyl substituent rather than the ethyl or isopropyl substituted side, *E* isomers were obtained as the major products. The 1:1 mixture of *E* and *Z* isomers was treated with gold catalyst to check the possibility of cyclization and subsequent isomerization, however, the ratio did not change. Thus, we theorized that the reaction would not be effectively controlled by the steric differences of the allene substituents in the coordinating process by the gold catalyst. High enantioselective excess (around 90 %) was obtained for each *E* or *Z* isomer, in accordance with the result of a nonbonding interaction between the amine nucleophile and gold catalyst.

To investigate the coordination geometry of the gold catalyst producing the unexpected *E/Z* ratio, the enantio-rich allene substrate **3c** (50 % ee) was treated with the [(*R*)-binap(AuOPNB)<sub>2</sub>] and [(*S*)-binap(AuOPNB)<sub>2</sub>] catalysts (Table 2). Both reactions predominantly afforded the *E* isomer as a major product in the ratio of approximately 2:1, which is an identical result to that of racemic allene as a starting material. This verifies that the two enantiomeric species might interconvert reversibly under the gold(I)-catalyzed reaction conditions.<sup>[6d, 20]</sup>

Table 2. Gold(I)-catalyzed enantioselective hydroamination of enantio-rich allenes.<sup>[a]</sup>

Precursor	L*	Product	Yield	<i>E/Z</i>	ee ( <i>E</i> )	ee ( <i>Z</i> )
<i>rac</i> - <b>3c</b>	( <i>R</i> )-binap	<b>4c</b>	95	2.0:1	78	88
( <i>S</i> )- <b>3c</b> <sup>[b]</sup>	( <i>R</i> )-binap	<b>4c</b>	97	2.0:1	81	90
( <i>S</i> )- <b>3c</b> <sup>[b]</sup>	( <i>S</i> )-binap	<i>ent</i> - <b>4c</b>	97	2.0:1	-82	-82

[a] Reaction conditions: 3 mol % L\*(AuOPNB)<sub>2</sub>, MeNO<sub>2</sub> (0.3 M), 50 °C. Yield (%) of isolated products (*E*+*Z*) after column chromatography.

[b] 50 % ee of (*S*)-**3c**.

Calculations were carried out for the intermediates of *(R)*-**4b/*(S)*-**4b and *(E)*-**4b/*(Z)*-**4b to elucidate the observed stereoselectivity in favor of the *S,E* isomer. We found that the intermediates of the *R,E* and *R,Z* isomers are much less favored than those of *S* isomers; this is consistent with our previous discussions for Figure 1. The pre-reaction complex towards *S,Z* isomer is calculated to be the most stable (energy (Gibbs free energy) is 2.0 (2.9) kcal mol<sup>-1</sup> lower than *S,E* isomer; Figure 3). However, the post-reaction complex towards *S,E* form is of slightly lower energy (by 0.8 kcal mol<sup>-1</sup>) and the resulting larger reaction Gibbs free energy  $\Delta G$  seems to make it more favored. This difference in Gibbs free energy could be understood by examining the Au–Au electrostatic interactions in *S,Z* and *S,E* isomers.<sup>[21]</sup>********

Although we tried to isolate the proposed catalytic intermediates (the vinyl gold complexes),<sup>[22]</sup> various treatments of allene substrates with a stoichiometric amount of gold catalyst either resulted in the allene substrate being recovered under low temperature, or the cyclized product obtained under higher temperature, even in the presence of base, indicating the relatively rapid protodeauration. Additional efforts to obtain the crystalline sample of pre-reaction complex, in which the gold catalyst is coordinated to the allenes, were also unsuccessful, although the <sup>1</sup>H NMR spectra showed that the allenic proton shifted downfield, thereby envisaging the formation of gold-coordinated allene.

In conclusion, we have presented the counterion-mediated *syn*-addition pathway in gold-catalyzed hydroamination reactions, and proved the bis(gold)-phosphine complex as the outstanding catalyst with the aurophilic Au–Au interaction. The strong interaction between the amine nucleophile and gold is found to be essential to enhance the enantioselectivity of complex allene substrates. This unprecedented mechanism will lead to a more profound insight into the gold-catalyzed reactions, thus showing the great counterion effects, as well as the transition metal catalyzed processes in general.

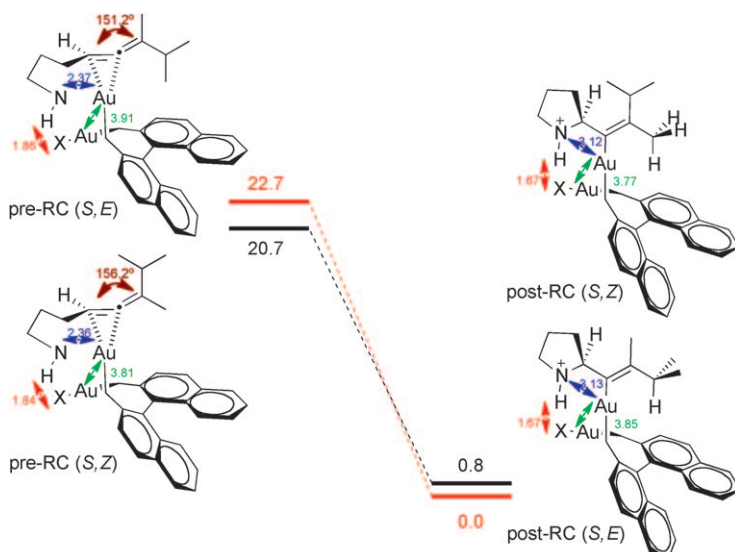


Figure 3. Energy profile for *E* and *Z* isomeric pathways. Distances in Å, and relative energies in kcal mol<sup>-1</sup>.

## Acknowledgements

This research was supported by Basic Science Research Program through the National Research Foundation of Korea (NRF) funded by the Ministry of Education, Science and Technology (2010-0013560) (E.J.K.), and the Ministry of Health, Welfare and Family Affairs of Korea, and the Ministry of Education, Science and Technology (Converging Research Program, 2009-0081952) (S.L.).

**Keywords:** allenes • counterions • gold • hydrogen bonds • nucleophilic addition

- [1] A. R. Chianese, S. J. Lee, M. R. Gagné, *Angew. Chem.* **2007**, *119*, 4118–4136; *Angew. Chem. Int. Ed.* **2007**, *46*, 4042–4059.
- [2] Ir-catalyzed reactions, see: a) A. L. Casalnuovo, J. C. Calabrese, D. Milstein, *J. Am. Chem. Soc.* **1988**, *110*, 6738–6744; b) J. Zhou, J. F. Hartwig, *J. Am. Chem. Soc.* **2008**, *130*, 12220–12221; Ln-catalyzed reactions, see: c) V. M. Arredondo, F. E. McDonald, T. J. Marks, *J. Am. Chem. Soc.* **1998**, *120*, 4871–4872; Pd-catalyzed reactions, see: d) M. Meguro, Y. Yamamoto, *Tetrahedron Lett.* **1998**, *39*, 5421–5424; Au-catalyzed reactions, see: e) J. H. Teles, S. Brode, M. Chabanas, *Angew. Chem.* **1998**, *110*, 1475–1478; *Angew. Chem. Int. Ed.* **1998**, *37*, 1415–1418; f) E. Mizushima, T. Hayashi, M. Tanaka, *Org. Lett.* **2003**, *5*, 3349–3352; g) N. Nishina, Y. Yamamoto, *Angew. Chem. Int. Ed.* **2006**, *118*, 3392–3395; *Angew. Chem. Int. Ed.* **2006**, *45*, 3314–3317; h) V. Lavallo, G. D. Frey, S. Kousar, B. Donnadieu, G. Bertrand, *Proc. Natl. Acad. Sci. USA* **2007**, *104*, 13569–13573; i) V. Lavallo, G. D. Frey, B. Donnadieu, M. Soleilhavoup, G. Bertrand, *Angew. Chem.* **2008**, *120*, 5302–5306; *Angew. Chem. Int. Ed.* **2008**, *47*, 5224–5228; j) X. Zeng, G. D. Frey, S. Kousar, G. Bertrand, *Chem. Eur. J.* **2009**, *15*, 3056–3060; k) X. Zeng, G. D. Frey, R. Kinjo, B. Donnadieu, G. Bertrand, *J. Am. Chem. Soc.* **2009**, *131*, 8690–8696.
- [3] a) A. Togni, S. D. Pastor, *Helv. Chim. Acta* **1989**, *72*, 1038–1042; b) G. Kovács, G. Ujaque, A. Lledós, *J. Am. Chem. Soc.* **2008**, *130*, 853–864; c) L.-P. Liu, B. Xu, M. S. Mashuta, G. B. Hammond, *J. Am. Chem. Soc.* **2008**, *130*, 17642–17643; d) N. Nishina, Y. Yamamoto, *Tetrahedron* **2009**, *65*, 1799–1808; e) R. S. Paton, F. Maseras, *Org. Lett.* **2009**, *11*, 2237–2240; f) G. Lemiere, V. Gandon, K. Cariou, A. Hours, T. Fukuyama, A.-L. Dhimane, L. Fensterbank, M. Malacia, *J. Am. Chem. Soc.* **2009**, *131*, 2993–3006; g) R. L. Londe, W. E. Brenzovich, Jr., D. Benitez, E. Tkatchouk, K. Kelley, W. A. Goddard, III, F. D. Toste, *Chem. Sci.* **2010**, *1*, 226–233; h) X. Zeng, R. Kinjo, B. Donnadieu, G. Bertrand, *Angew. Chem.* **2010**, *122*, 954–957; *Angew. Chem. Int. Ed.* **2010**, *49*, 942–945; i) D. Gayralade, E. Gómez-Benagoa, X. Huang, A. Goede, C. Nevado, *J. Am. Chem. Soc.* **2010**, *132*, 4720–4730; j) R.-X. Zhu, D.-J. Zhang, J.-X. Guo, J.-L. Mu, C.-G. Duan, C.-B. Liu, *J. Phys. Chem. A* **2010**, *114*, 4689–4696; k) A. S. K. Hashmi, *Angew. Chem.* **2010**, *122*, 5360–5369; *Angew. Chem. Int. Ed.* **2010**, *49*, 5232–5241; l) Z. J. Wang, D. Benitez, E. Tkatchouk, W. A. Goddard, III, F. D. Toste, *J. Am. Chem. Soc.* **2010**, *132*, 13064–13071; m) C. M. Krauter, A. S. K. Hashmi, M. Pernpoint-

## COMMUNICATION

- ner, *ChemCatChem* **2010**, *2*, 1226–1230; n) M.-Z. Wang, C.-Y. Zhou, Z. Guo, E. L.-M. Wong, M.-K. Wong, C.-M. Che, *Chem. Asian J.* **2011**, *6*, 812–824.
- [4] For gold-catalyzed hydrofunctionalization reactions of allenes (racemic examples), see: a) C.-Y. Zhou, P. W. H. Chan, C.-M. Che, *Org. Lett.* **2006**, *8*, 325–328; b) Z. Zhang, C. Liu, R. E. Kinder, X. Han, H. Qian, R. A. Widenhoefer, *J. Am. Chem. Soc.* **2006**, *128*, 9066–9073; c) R. A. Widenhoefer, X. Han, *Eur. J. Org. Chem.* **2006**, 4555–4563; d) C. J. T. Hyland, L. S. Hegedus, *J. Org. Chem.* **2006**, *71*, 8658–8660; e) J. Piera, P. Krumlinde, D. Strübing, J.-E. Bäckvall, *Org. Lett.* **2007**, *9*, 2235–3327; f) R. E. Kinder, Z. Zhang, R. A. Widenhoefer, *Org. Lett.* **2008**, *10*, 3157–3159; g) N. Nishina, Y. Yamamoto, *Tetrahedron Lett.* **2008**, *49*, 4908–4911; h) A. M. Manzo, A. D. Perboni, G. Broggini, M. Rigamonti, *Tetrahedron Lett.* **2009**, *50*, 4696–4699; i) X. Zeng, M. Soleilhavoup, G. Bertrand, *Org. Lett.* **2009**, *11*, 3166–3169; j) A. N. Duncan, R. A. Widenhoefer, *Synlett* **2010**, *3*, 419–422; for chirality transfer reactions, see: k) N. Morita, N. Krause, *Angew. Chem.* **2006**, *118*, 1930–1933; *Angew. Chem. Int. Ed.* **2006**, *45*, 1897–1899; l) N. T. Patil, L. M. Lutete, N. Nishina, Y. Yamamoto, *Tetrahedron Lett.* **2006**, *47*, 4749–4751; m) N. Morita, N. Krause, *Eur. J. Org. Chem.* **2006**, 4634–4641; n) C. Deutsch, B. Gockel, A. Hoffmann-Röder, N. Krause, *Synlett* **2007**, *11*, 1790–1794; o) Z. Zhang, R. A. Widenhoefer, *Org. Lett.* **2008**, *10*, 2079–2081.
- [5] For other transition metal-catalyzed hydroamination of allenes, see: a) A. S. K. Hashmi, *Angew. Chem.* **2000**, *112*, 3737–3740; *Angew. Chem. Int. Ed.* **2000**, *39*, 3590–3593; b) C. Jonasson, A. Horváth, J.-E. Bäckvall, *J. Am. Chem. Soc.* **2000**, *122*, 9600–9609; c) A. Tsuhako, D. Oikawa, K. Sakai, S. Okamoto, *Tetrahedron Lett.* **2008**, *49*, 6529–6532.
- [6] For enantioselective hydrofunctionalization of allenes, see: a) Z. Zhang, R. A. Widenhoefer, *Angew. Chem.* **2007**, *119*, 287–289; *Angew. Chem. Int. Ed.* **2007**, *46*, 283–285; b) R. L. LaLonde, B. D. Sherry, E. J. Kang, F. D. Toste, *J. Am. Chem. Soc.* **2007**, *129*, 2452–2453; c) M. A. Tarselli, A. R. Chianese, S. J. Lee, M. R. Gagné, *Angew. Chem.* **2007**, *119*, 6790–6793; *Angew. Chem. Int. Ed.* **2007**, *46*, 6670–6673; d) Z. Zhang, C. F. Bender, R. A. Widenhoefer, *J. Am. Chem. Soc.* **2007**, *129*, 14148–14149; e) C. Liu, R. A. Widenhoefer, *Org. Lett.* **2007**, *9*, 1935–1938; f) Z. Zhang, C. F. Bender, R. A. Widenhoefer, *Org. Lett.* **2007**, *9*, 2887–2889; g) R. L. LaLonde, Z. J. Wang, M. Mba, A. D. Lackner, F. D. Toste, *Angew. Chem.* **2010**, *122*, 608–611; *Angew. Chem. Int. Ed.* **2010**, *49*, 598–601; h) C. Bartolomé, D. García-Cuadrado, Z. Ramiro, P. Espinet, *Inorg. Chem.* **2010**, *49*, 9758–9764.
- [7] For the selected reviews of enantioselective gold(I) catalysis, see: a) D. J. Gorin, B. D. Sherry, F. D. Toste, *Chem. Rev.* **2008**, *108*, 3351–3378; b) R. A. Widenhoefer, *Chem. Eur. J.* **2008**, *14*, 5382–5391; c) H. C. Shen, *Tetrahedron* **2008**, *64*, 3885–3903; d) Z. Li, C. Brouwer, C. He, *Chem. Rev.* **2008**, *108*, 3239–3265.
- [8] a) H. Schmidbaur, W. Graf, G. Müller, *Angew. Chem.* **1988**, *100*, 439–441; *Angew. Chem. Int. Ed. Engl.* **1988**, *27*, 417–419; b) P. Pykkö, Y. Zhao, *Angew. Chem.* **1991**, *103*, 622–623; *Angew. Chem. Int. Ed. Engl.* **1991**, *30*, 604–605; c) P. Pykkö, *Angew. Chem.* **2004**, *116*, 4512–4557; *Angew. Chem. Int. Ed.* **2004**, *43*, 4412–4456; d) H. Schmidbaur, A. Schier, *Chem. Soc. Rev.* **2008**, *37*, 1931–1951; e) R. J. Puddephatt, *Chem. Soc. Rev.* **2008**, *37*, 2012–2027.
- [9] a) C. Lee, W. Yang, R. P. Parr, *Phys. Rev. B* **1988**, *37*, 785–789; b) A. D. Becke, *J. Chem. Phys.* **1993**, *98*, 5648–5652.
- [10] P. J. Hay, W. R. Wadt, *J. Chem. Phys.* **1985**, *82*, 299–310.
- [11] M. J. Frisch, et al., Gaussian 09, Gaussian, Inc., Wallingford CT, **2009**.
- [12] a) G. L. Hamilton, E. J. Kang, M. Mba, F. D. Toste, *Science* **2007**, *317*, 496–499; b) K. Aikawa, M. Kojima, K. Mikami, *Angew. Chem.* **2009**, *121*, 6189–6193; *Angew. Chem. Int. Ed.* **2009**, *48*, 6073–6077.
- [13] Undisclosed result of 10% ee in the reaction with (*S*)-MOP-(AuOPNB) (MOP; axially chiral monophosphine ligand) also supported the important role of the coordinated counteranion and Au–Au interaction. Similar result, see: J. J. Kennedy-Smith, S. T. Staben, F. D. Toste, *J. Am. Chem. Soc.* **2004**, *126*, 4526–4527.
- [14] The shorter hydrogen-bond distance (1.89 Å) and Au–Au distance (3.50 Å) in the pre-reaction complex of tosyl amide substrate confirm the similar bonding effects as the key binding force. See the Supporting Information for the detailed comparison.
- [15] a) L. S. Hollis, S. L. Lippard, *J. Am. Chem. Soc.* **1983**, *105*, 4293–4299; b) R. Arumunto, C. F. Schwenk, B. M. Rode, *J. Am. Chem. Soc.* **2004**, *126*, 9934–9935.
- [16] Snapshots and an energy profile from a conformation, in which the amino group is located in the *anti* position to allene, are described in the Supporting Information.
- [17] These bent allene transition states (TS (*S*) and TS (*R*)) showed the unsymmetric C2-coordinated pattern, thus leading to be closer to C1(amino alkyl substituted) than C3 (cyclohexyl substituted); for TS (*S*),  $\chi(\text{Au}–\text{C}2–\text{C}1)=98.1^\circ$ ,  $\chi(\text{Au}–\text{C}2–\text{C}3)=123.0^\circ$ ; for TS (*R*),  $\chi(\text{Au}–\text{C}2–\text{C}1)=101.4^\circ$ ,  $\chi(\text{Au}–\text{C}2–\text{C}3)=122.6^\circ$ .
- [18] A. Johnson, R. J. Puddephatt, *J. Chem. Soc. Dalton Trans.* **1978**, 980–985.
- [19] It is noteworthy that this is an opposite result to the one catalyzed by [(*S*)-3,5-*t*Bu-4-MeO-MeObiphep(AuCl)] (*S*)-2,2'-bis[di(3,5-di-*tert*-butyl-4-methoxyphenyl)phosphino]-6,6'-dimethoxy-1,1'-biphenyl (biphep) (2.5 mol %) and AgClO<sub>4</sub> (5 mol %) in favor of the *Z* isomers.<sup>[6d]</sup>
- [20] a) B. Sherry, F. D. Toste, *J. Am. Chem. Soc.* **2004**, *126*, 15978–15979; b) V. Gandon, G. Lemière, A. Hours, L. Fensterbank, M. Malacria, *Angew. Chem.* **2008**, *120*, 7644–7648; *Angew. Chem. Int. Ed.* **2008**, *47*, 7534–7538.
- [21] The NBO (natural bond orbital) charges of the allene-coordinated Au atom and the other Au atom in the *S,E* isomer are 0.126 and 0.345 and in the *S,Z* isomer are 0.135 and 0.343, and the  $R_{\text{Au}–\text{Au}}$  distance in the *S,E* isomer is 3.853 Å and in the *S,Z* isomer is 3.765 Å. The resulting Au–Au Coulombic repulsion energy in the *S,E* isomer is about 4% smaller than in the *S,Z* isomer, and this slightly smaller Au–Au repulsion seems to account for the enhanced stability of the *S,E* isomer.
- [22] For some investigations on vinyl gold(I) compounds, see: a) L. P. Liu, G. B. Hammond, *Chem. Asian J.* **2009**, *4*, 1230–1236; b) D. Weber, M. A. Tarselli, M. R. Gagné, *Angew. Chem.* **2009**, *121*, 5843–5846; *Angew. Chem. Int. Ed.* **2009**, *48*, 5733–5736; c) A. S. K. Hashmi, A. M. Schuster, F. Rominger, *Angew. Chem.* **2009**, *121*, 8396–8398; *Angew. Chem. Int. Ed.* **2009**, *48*, 8247–8249; d) A. S. K. Hashmi, T. D. Ramamurthy, F. Rominger, *Adv. Synth. Catal.* **2010**, *352*, 971–975.

Received: February 10, 2011  
Published online: July 6, 2011